Preliminary Validation using *in vivo* Measures of a Macroscopic Electrical Model of the Heart

M. Sermesant*[1], O. Faris[2], F. Evans[2], E. McVeigh[2], Y. Coudière[3], H. Delingette[1], and N. Ayache[1]

[1] Epidaure Research Project, INRIA Sophia Antipolis
2004 route des Lucioles, 06902 Sophia Antipolis, France
[2] National Institutes of Health, National Heart Lung and Blood Institute, Laboratory of Cardiac Energetics, Bethesda, Maryland
[3] Mathematics Laboratory, CNRS (UMR 6629), Nantes University
*Corresponding Author: Maxime.Sermesant@inria.fr

Abstract. This article describes an experimental protocol to obtain *in vivo* macroscopic measures of the cardiac electrical activity in a canine heart coupled with simulations done using macroscopic models of the canine myocardium. Electrical propagation simulations are conducted along with preliminary qualitative comparisons. Two different models are compared, one built from dissection and highly smoothed and one measured from Diffusion Tensor Imaging (DTI). We believe that validating a macroscopic model with *in vivo* measurements of the electrical activity should allow a future use of the model in a predictive way, for instance in radio-frequency ablation planning.

1 Introduction

Cardiac electrical activity disorders are involved in many pathologies, so simulating this activity could help to better understand these pathologies, guide diagnosis or plan interventions, like radio-frequency ablation. Direct *in vivo* measures are really necessary to improve knowledge of this phenomenon and macroscopic measures on the same heart start being possible [8].

But these measures are difficult to obtain and invasive. Coupling such measures with a model allows to validate the model and adjust its parameters. Once validated, a possible outcome is to use the model in a predictive way and to interpolate data where not available.

This article presents a protocol to measure electrical potentials on the epicardium and a macroscopic model of the myocardium electrical activity, along with simulated results of electrical propagation.

The chosen model is simple enough so that the parameters can be adjusted from macroscopic measures, at first qualitatively, and then quantitatively. As the number of unknowns is mush more important than the number of measures, a more complex model would not be tractable.

Moreover, we are more interested in studying the differences between the pathological and normal functions than precisely studying quantitatively a given function.

And it has to be computationally fast in order to be used as a simulator. The final goal is to use it in a predictive way and simulate pathologies, so it must be efficient enough to be used interactively.

In this paper, a qualitative adjustment of the model to the data is first performed, more quantitative adjustment is a work in progress.

2 Materials and Methods

2.1 Surgery and Experimental Layout

An adult male mongrel dog was used in this measure study. Anesthesia was induced with an initial intravenous injection of thiopental (25 mg/ml at 0.5ml/kg) and maintained after endotracheal intubation with isoflurane (0.8-2%, Siemens ventilator, 900D). A median sternotomy was performed, and a pericardial cradle was fashioned.

A multi-electrode epicardial sock consisting of a nylon mesh and 128 copper electrodes attached in an ordered fashion was then placed over the ventricular epicardium. The sock was placed in a consistent and pre-determined orientation and secured with several sutures (see fig. 1). Bipolar epicardial twisted-pair pacing electrodes were sewn onto the right atrium (RA). Similar electrodes were sewn onto the RV free-wall. A ground reference electrode was sewn onto the fat pad at the root of the aorta.

All sock and pacing wires were run directly out of the chest and connected, via a customized connection box, to two 64-channel analog to digital converter (A/D) boards (Hewlett-Packard, now Agilent, E1413C). All A/D boards were connected via FireWire (IEEE 1394) to a computer (Windows NT, 4.0) running data acquisition software (Hewlett-Packard, VEE 5.0).

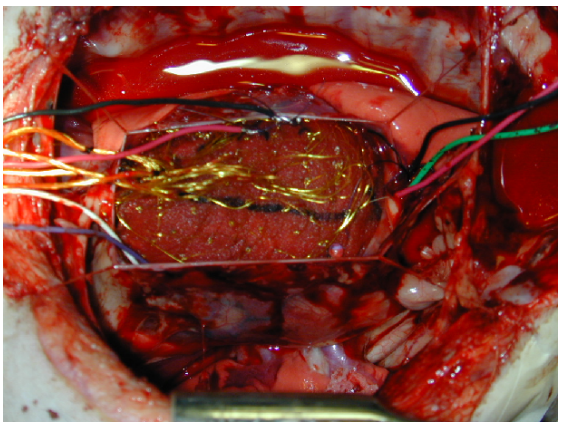

Fig. 1. Multi-electrode epicardial sock on the canine heart studied, *in vivo*.

2.2 Data Acquisition

RV pacing capture was established at a pacing rate (110-125 bpm) approximately 10-20% above intrinsic rate. Pacing current was set to approximately

20% above that needed for capture. Intrinsic electrical activation was suppressed by simultaneously pacing the RA and unipolar epicardial electrical recordings were obtained.

Electrical recordings were obtained at an acquisition rate of 1000-1450 Hz for a duration of approximately 10 seconds immediately prior to and following MR scans. Unipolar signals were electrically referenced to the aortic ground electrode.

After all *in vivo* image data and electrical recordings were obtained, the animal was heparinized and then euthanized with a bolus of potassium chloride while still under general anesthesia. The heart was excised with the sock still in place. The coronary arteries were then perfused from the aorta with isotonic saline at 50-60 mmHg to induce tissue turgor, and the heart was submerged in an isotonic saline bath to reduce body force deformation.

With the excised heart therefore in an approximate end-diastolic configuration, the LV and RV were then filled with vinyl polysiloxane by injection through the corresponding atria and atrioventricular valves to fix the shape. After approximately ten minutes, the vinyl polysiloxane solidified (see fig. 2). Using a 3D digitizer, the sock electrodes and localization markers were localized (digitizer coordinates). Additionally, locations of anatomical landmarks such as inter-ventricular sulcus, apex and aortic root were recorded.

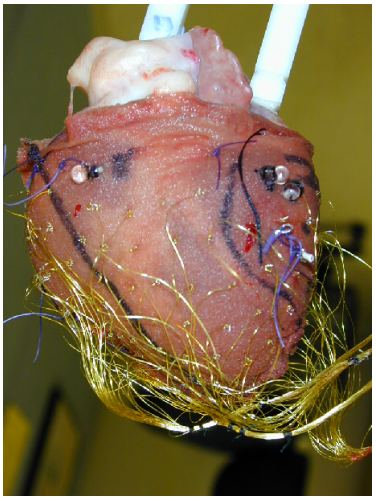

Fig. 2. Sock on the canine heart studied, once excised and polysiloxane-filled.

2.3 Data Analysis

For analysis of electrical activation, epicardial readings from each electrode were averaged over approximately 20 heartbeats. The five-point finite difference estimate of the derivative of the recorded voltage, v, as a function of time, t, was used:

$$\frac{dv(t)}{dt} = \frac{1}{12\Delta t}[-v(t+2\Delta t) + 8v(t+\Delta t) - 8v(t-\Delta t) + v(t-2\Delta t)]$$

Electrical activation times, referenced to the pacing stimulus, were chosen as the point of the most negative derivative, indicating the time of local depolarization. Due to pacing artifact, the first ten milliseconds after pacing were not used for the detection of activation times.

3 Heart Myocardium Modeling

The whole process used to build a model of the myocardium from different imaging modalities is more precisely detailed in [10]. As the anisotropy created by the muscle fibers intervenes in the electrical wave propagation (and in the mechanical contraction), we need to include these directions in the mesh.

For the presented simulations, we built two different models. One from a canine heart dissection done in the Bioengineering Institute, Auckland University, New Zealand[1], where position and fiber directions were measured. These fiber directions from Auckland were interpolated and smoothed by the Cardiac Mechanics Research Group[2], UCSD, United States, and we use the latest version, which is available as a vector 3D image of the fiber directions.

The other model is built from a canine heart Diffusion Tensor Imaging done in the Duke University Medical Center[3], North Carolina, United States, which directly gives an estimate of the fiber directions for each voxel of the image [7].

3.1 Geometry of the myocardium

For both models, we had the geometry in a 3D image format. To build the mesh from a 3D image, we extract the triangulated surface from the thresholded image, after using preprocessing like anisotropic diffusion and/or mathematical morphology to obtain a smooth binary mask.

As the quality of the tetrahedra depends on the quality of the surface (the surface stay unchanged when the inner volume is meshed), we improve the triangulation quality, using the INRIA Yams[4] software, by optimizing the triangles positions depending on the curvature of the mesh.

Finally, we mesh the volume with regularly sized tetrahedra to prevent smaller tetrahedra from reducing the stability of the time integration, using the INRIA Ghs3d[5] software. The presented models have around 8000 vertices and 40 000 tetrahedra.

To adapt the shape of the model to the geometry of the electrodes basket, an affine registration is computed between the surface nodes of the model and electrode points positions obtained from 3D digitizer, as described in section 4.3.

3.2 Fiber Directions

The data from reduced-encoding MR Diffusion Tensor Imaging (DTI) of a canine heart is quite noisy compared to the data from UCSD, see fig. 3. Such studies can

[1] http://www.bioeng.auckland.ac.nz/home/home.php
[2] http://cmrg.ucsd.edu/
[3] http://wwwcivm.mc.duke.edu/civmPeople/HsuEW/EWHsu.html
[4] http://www-rocq.inria.fr/gamma/yams/
[5] http://www-rocq.inria.fr/gamma/ghs3d/

help compare the results obtained with this modality with the results obtained with a smoothed model. We assign the fiber directions to the tetrahedral mesh

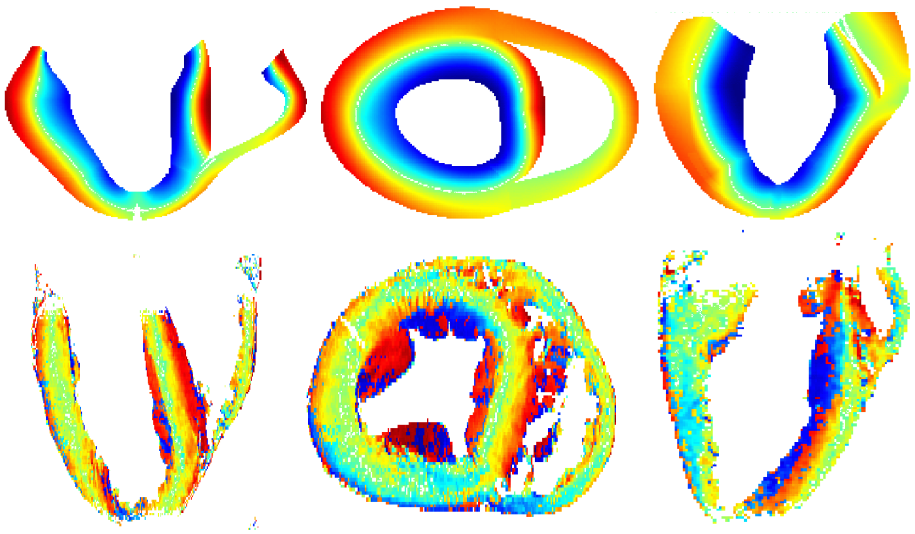

Fig. 3. Elevation angle of the fiber directions. (Top) 3 slices from a 3D image of the interpolated values representing the cardiac muscle fiber directions (data courtesy of A. McCulloch *et al.*). (Bottom) 3 slices from a 3D diffusion tensor MRI representing the cardiac muscle fiber directions (DTI data courtesy of Dr. Hsu *et al.*).

using the rasterization procedure detailed in [10] (see fig. 4).

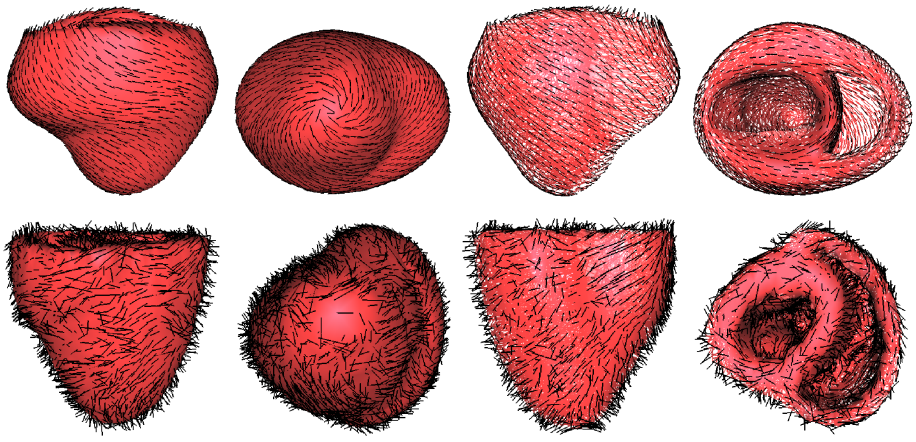

Fig. 4. Fiber directions assigned to the myocardium mesh from the UCSD interpolated data (top) and DTI data (bottom), anterior and posterior views.

4 Electrical Model

4.1 Cell Level

At the cell level, the main idea is to study the relationship between the transmembrane ionic currents and the ionic potentials inside and outside the cell. The models concerning this relation improve while the number of phenomena observed at the cell level increases [3].

At the beginning, we are only concerned with a model expected to account for the most important biological phenomena:

- a cell is activated only for a stimulus larger than a certain threshold;
- the shape of the action potential does not depend on the stimulus (it is only model-dependent);
- there is a refractory period during which the cell cannot be excited;
- a cell can act as a pacemaker.

Different models are available for such a simulation. Luo-Rudy models include many ionic currents to model precisely the evolution of the potentials. To be able to adjust the model from macroscopic measures, we chose a more global model where the variables are directly macroscopic potentials.

In so-called bidomain models, extra-cellular *and* intra-cellular potentials are included. We chose a mono-domain model, where we only compute the action potential (which is the difference between the two previously cited potentials) as the primary objective of computing this electrical potential is to control an electro-mechanical coupling, and the contraction is controlled by the action potential.

A FitzHugh like model [5] seems to correctly capture these behaviors, and yields fast 3D computations. Aliev and Panfilov developed a modified version of the FitzHugh-Nagumo equations adapted to the dynamic of the cardiac electrical potential [1]. We simplified this model, as the complete ε term is mainly useful to model the influence of changes in pacing frequency and we do not need this behavior for the moment. Here is the set of differential equation studied:

$$\begin{aligned} \partial_t u &= ku(1-u)(u-a) - uz \\ \partial_t z &= -\varepsilon(ku(u-a-1) + z)) \end{aligned} \tag{1}$$

u is a normalized potential and z is a dynamic variable modeling the repolarization. k and ε control the repolarization, and a the reaction phenomenon. Parameters values are taken from [1].

With an excitation above the initialization threshold, the simulated action potential with this system is rather similar to measurements of cardiac action potentials (fig. 5).

4.2 Whole Ventricle Level – Anisotropy

At the macroscopic scale, the ventricles are considered as a conducting continuum, where the local potentials are undergoing at the same time the diffusion

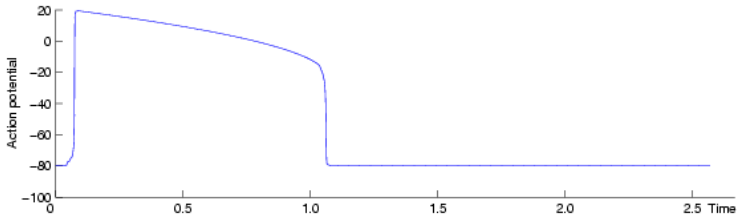

Fig. 5. 1D measure of action potential simulation with simplified Aliev and Panfilov model.

and the reaction phenomena described by the models above. Hence, (1) becomes:

$$\begin{aligned} \partial_t u &= \operatorname{div}(D\nabla(u)) + ku(1-u)(u-a) - uz \\ \partial_t z &= -\varepsilon(ku(u-a-1)+z)) \end{aligned} \tag{2}$$

On a physiological point of view, these equations are understood either as a mathematical approximation of the dynamical system introduced by Hodgkin and Huxley [6], as in [5], or as the result of some equilibrium equations that govern the conducting continuum, like in the bidomain model [11].

The anisotropy of the ventricles is taken into account through the diffusion tensor D: $D = d_0.diag(1, \rho, \rho)$, in a local orthonormal basis ($\mathbf{i}$, $\mathbf{j}$, $\mathbf{k}$) where $\mathbf{i}$ is parallel to the fiber. d_0 is a scalar conductivity and ρ the anisotropy ratio between the transverse and the axial conductivities. It is typically said that the electrical propagation goes two times faster in the fiber direction, so the used value is $\rho = 0.5$ (and $d_0 = 1.0$, as the system is adimensioned).

Once adimensioned with x and t between 0 and 1, the system is dimensioned spatially to the max dimension of the mesh and temporally so that the action potential duration is around 0.3 s ($\tau = 0.26t$, with τ the dimensioned time and t the computational time). The other parameters are: $\varepsilon = 0.01$, $k = 8.0$, $a = 0.15$.

To initiate the action potential propagation, we need to locate the extremities of the Purkinje network, the specialized system that conducts the depolarization from the atrio-ventricular node to the myocardium.

The Purkinje network is hardly visible by dissection and by imaging. We used the measures from Durrer *et al.* [4] to locate the Purkinje network extremities on the endocardia of both the left and right ventricles (the version of [4] presented here (fig. 6) was found on the web[6]).

We then first validated the 3D computation by comparing the resulting action potential isochrones with the measures from Durrer *et al.* (see fig. 6). The temporal integration is done with explicit Euler scheme and the spatial integration is done with linear tetrahedral elements. The computation time step is 10^{-5} and a 3D simulation takes around half an hour on a standard PC with 40 000 elements.

From the qualitative comparison between the resulting simulations, we can observe that both models seem to reproduce the activation patterns visible on

[6] `http://butler.cc.tut.fi/~malmivuo/bem/bembook/`

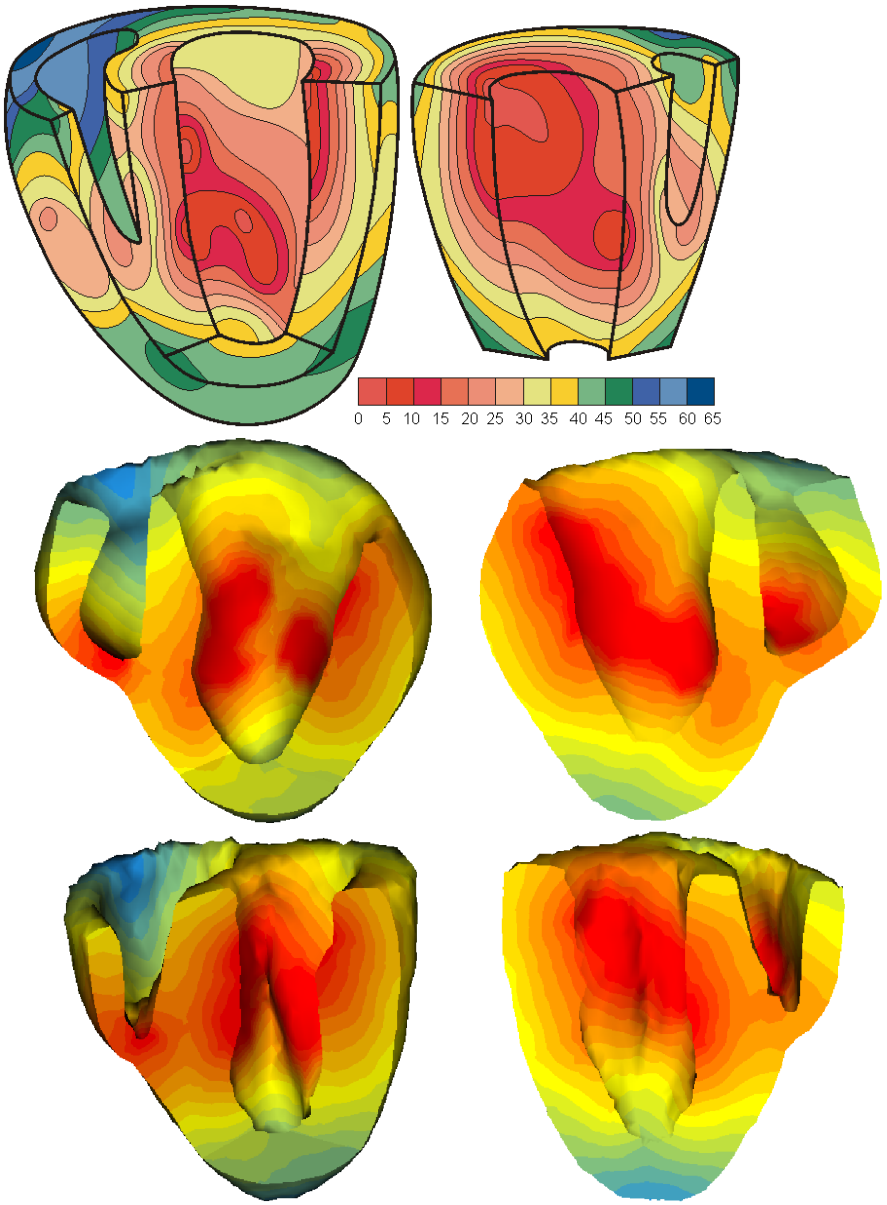

Fig. 6. Action potential isochrones measured by Durrer *et al.* (top row) compared with the simulated ones using the model built from UCSD data (middle row) and from DTI (bottom row).

the measures, with maybe a closer result for the smoother model. But as the activation initialization is not exactly at the same place, due to anatomical differences, a more detailed comparison is difficult. This is another reason why measures with precisely located pacing electrodes are very valuable.

To try to evaluate the effect of anisotropy, simulations were conducted using an isotropic diffusion tensor (see fig. 7). As the fibers have quite a small radial component, the diffusion in the wall is much slower in the anisotropic case. And

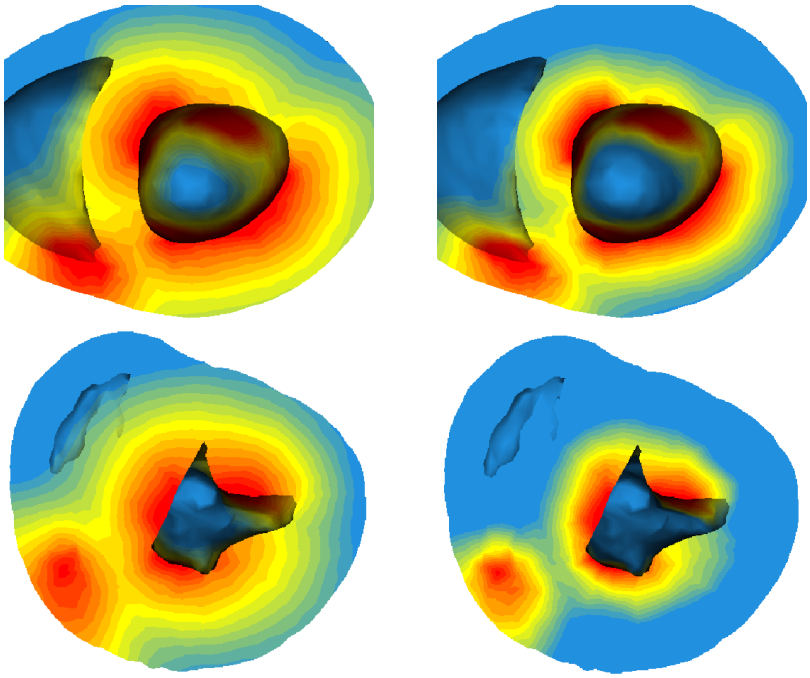

Fig. 7. Comparison between isotropic (left) and anisotropic (right) propagation for the model built from UCSD data (top row) and from DTI (bottom row). The fibers are mainly circumferential, so the radial diffusion is much slower with anisotropy.

the anisotropy effect seems more important with the model built from DTI. As the fiber directions are noisier, there are more discontinuities, so the propagation is more affected by the anisotropy.

4.3 Simulation of the *in vivo* Measurements

Model Geometry We have the 3D position of the electrodes plus different points on the left ventricle endocardium. We fitted surfacic meshes to these point clouds to interpolate the positions and have more 3D data to register. These surfaces were transformed into binary 3D images. And we then compute an affine transformation between the models built and the myocardium image created from the measures, using the hierarchical method described in [10].

Ultimately, the model geometry will be fitted to the data geometry directly in a 3D image of the measured heart, using the method described in [10] to obtain local deformations.

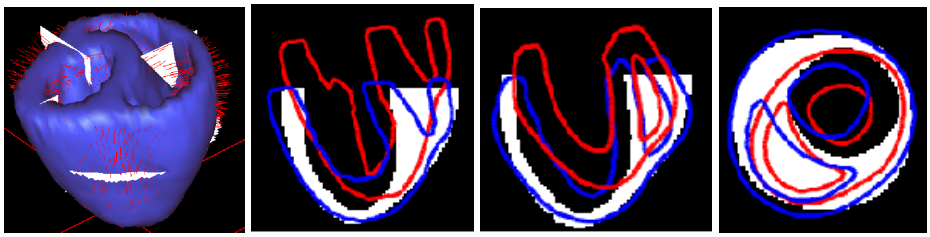

Fig. 8. Affine registration between the two models built and a 3D Image created from the position of the electrodes and points on the left ventricle endocardium. (left) matching between the model and the image voxels. (others) initial position in red and final position in blue.

Simulated pacing In order to complete our anatomical model we also need data about electrical onset areas of the ventricular depolarization. In the presented measures, the location of the pacing electrodes is well known, which is very interesting for simulating propagation.

Pacing electrodes are simulated by imposing an initial action potential in the epicardium location corresponding to the localization of the pacing electrodes in the measure protocol, see fig. 9.

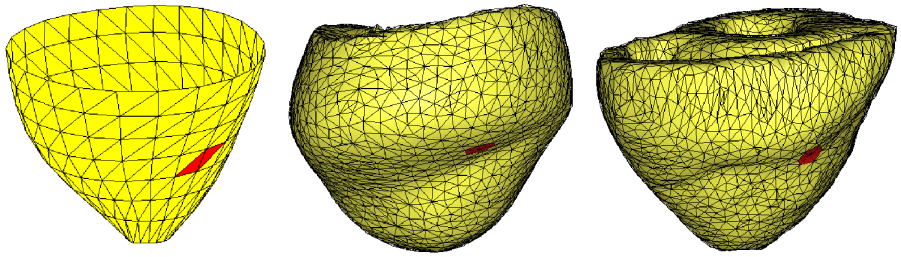

Fig. 9. Red triangles: real (left) and simulated pacing electrode location (middle: UCSD model, right: DTI model).

4.4 Results of the wave propagation

We simulated the propagation of the action potential in the 3D meshes of the myocardium constructed, initiating the wave at the location defined in previous section. Fig. 10 presents resulting simulated isochrones of activation.

As we compute the action potential and not both intra-cellular and extra-cellular potentials, we cannot compare the electrical measures directly with our simulations, we can only compare the activation times, through the isochrones.

The results look qualitatively good and using a 3D propagation model allows also to visualize the simulated potential inside the myocardium wall (see fig. 11).

We can observe that in the model from DTI, the discontinuities in the fiber directions in the right ventricle create a delay in the electrical propagation, and the dissymmetry in the propagation does not seem to be present in the measures.

We can think that due to the noise in the current *in vivo* measurements in fiber directions, it could be preferable to use a smoothed model rather than measures from another heart.

Ultimately, the DTI image will be from the same canine heart as the measures (there are ongoing DTI measurements on the heart of the experiment), so we will be able to determine whether the simulations with a specific model can give better results than ones with a general smoothed model.

5 Conclusion and Perspectives

We presented in this article first qualitative results comparing measures and simulations of the electrical activity of a canine heart. The smoothed model seems to capture well the behavior of the electrical propagation.

Quantitative adjustment of the parameters of the model are an ongoing work, using data assimilation techniques based on Kalman filtering but no existing method is really suited to adjust such a model with this kind of data. Ultimately, such a model could allow to find electrical activity patterns directly from ECG measures.

This time-dependent computed potential can also be used as an excitation entry to the system describing the mechanical behavior of the myocardium, as we developed a model of the electro-mechanical coupling [9]. Tagged cine images acquired during RV pacing in this study are very useful for this task.

Indeed, we can compute nodes displacements from the electro-mechanical coupling, and compare these displacements with the displacement extracted from MRI.

Once the whole model has been validated, it can be used in a predictive way to study pathologies and intervention planning.

6 Acknowledgements

The modeling and data assimilation work is a part of the multidisciplinary project ICEMA[7] (standing for Images of the Cardiac Electro-Mechanical Activity) and ICEMA-2[8], which are collaborative research actions between different INRIA projects and Philips Research France [2].

All aspects of this study were conducted in accordance with the guidelines of the Animal Care and Use Committee of the National Heart, Lung, and Blood Institute.

[7] `http://www-rocq.inria.fr/who/Frederique.Clement/icema.html`
[8] `http://www-rocq.inria.fr/sosso/icema2/icema2.html`

Additional color version of the images and videos can be found on the web[9].

References

1. R. Aliev and A. Panfilov. A simple two-variable model of cardiac excitation. *Chaos, Solitons & Fractals*, 7(3):293–301, 1996.
2. N. Ayache, D. Chapelle, F. Clément, Y. Coudière, H. Delingette, J.A. Désidéri, M. Sermesant, M. Sorine, and J. Urquiza. Towards model-based estimation of the cardiac electro-mechanical activity from ECG signals and ultrasound images. In *Functional Imaging and Modeling of the Heart (FIMH'01)*, number 2230 in Lecture Notes in Computer Science (LNCS), pages 120–127. Springer, 2001.
3. A. L. Bardou, P. M. Auger, P. J. Birkui, and J.-L. Chassé. Modeling of cardiac electrophysiological mechanisms: From action potential genesis to its propagation in myocardium. *Critical Reviews in Biomedical Engineering*, 24:141–221, 1996.
4. D. Durrer, R.T. van Dam, G.E. Freud, M.J. Janse, F.L. Meijler, and R.C. Arzbaecher. Total excitation of the isolated human heart. *Circulation*, 41(6):899–912, 1970.
5. R.A. FitzHugh. Impulses and physiological states in theoretical models of nerve membrane. *Biophysical Journal*, 1:445–466, 1961.
6. A.L. Hodgkin and A.F. Huxley. A quantitative description of membrane current and its application to conduction and excitation in nerve. *Journal of Physiology*, 177:500–544, 1952.
7. E. Hsu and C. Henriquez. Myocardial fiber orientation mapping using reduced encoding diffusion tensor imaging. *Journal of Cardiovascular Magnetic Resonance*, 3:325–333, 2001.
8. E. McVeigh, O. Faris, D. Ennis, P. Helm, and F. Evans. Measurement of ventricular wall motion, epicardial electrical mapping, and myocardial fiber angles in the same heart. In *Functional Imaging and Modeling of the Heart (FIMH'01)*, number 2230 in Lecture Notes in Computer Science (LNCS), pages 76–82. Springer, 2001.
9. M. Sermesant, Y. Coudière, H. Delingette, N. Ayache, J. Sainte-Marie, D. Chapelle, F. Clément, and M. Sorine. Progress towards model-based estimation of the cardiac electromechanical activity from ECG signals and 4D images. In *Modelling & Simulation for Computer-aided Medicine and Surgery (MS4CMS'02)*, 2002.
10. M. Sermesant, C. Forest, X. Pennec, H. Delingette, and N. Ayache. Biomechanical model construction from different modalities: Application to cardiac images. In *Medical Image Computing and Computer-Assisted Intervention (MICCAI'02)*, volume 2208 of *Lecture Notes in Computer Science (LNCS)*, pages 714–721. Springer, 2002.
11. K. Simelius, J. Nenonen, and B.M. Horácek. Simulation of anisotropic propagation in the myocardium with a hybrid bidomain model. In *Functional Imaging and Modeling of the Heart (FIMH'01)*, number 2230 in Lecture Notes in Computer Science (LNCS), pages 140–147. Springer, 2001.

[9] `http://www-sop.inria.fr/epidaure/personnel/Maxime.Sermesant/gallery.php`

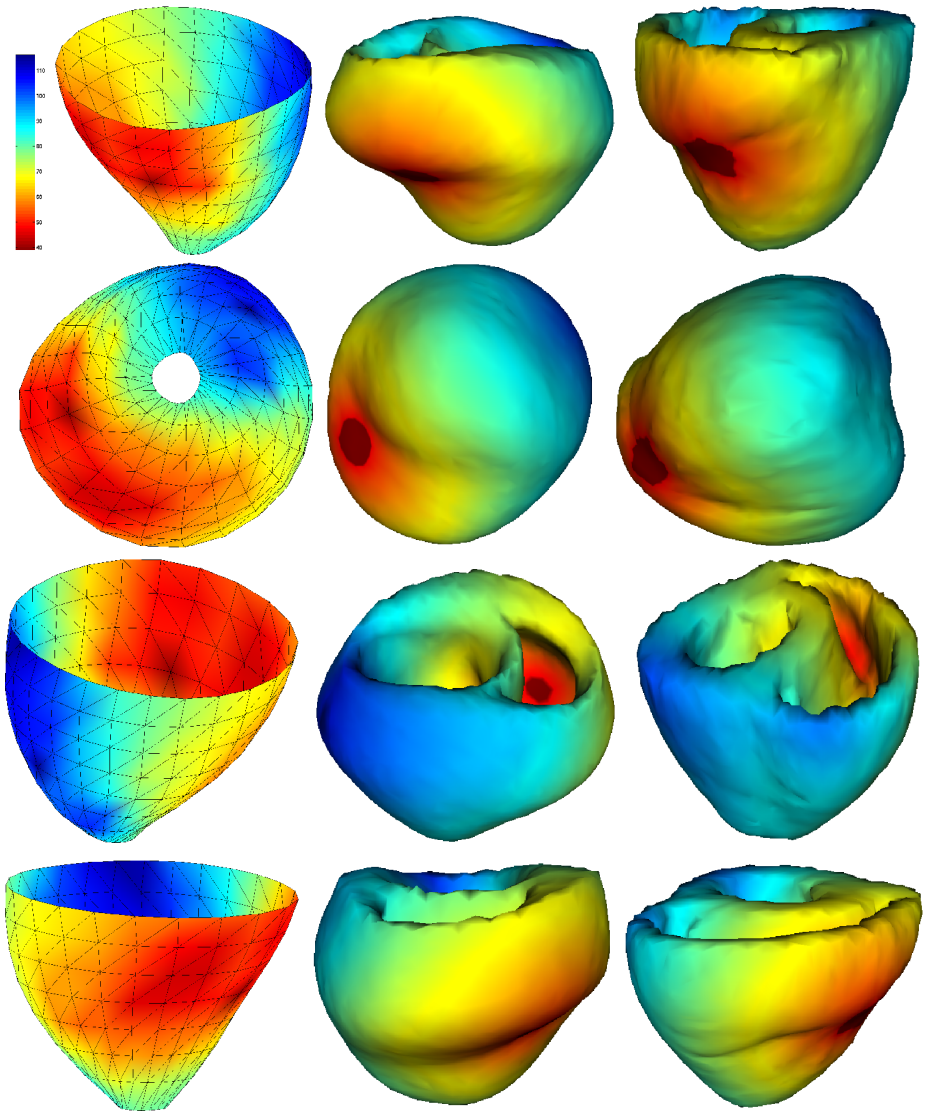

Fig. 10. Measured and Simulated Action Potential isochrones. Left: measures, middle: simulation with the UCSD model, right: simulation with the DTI model.

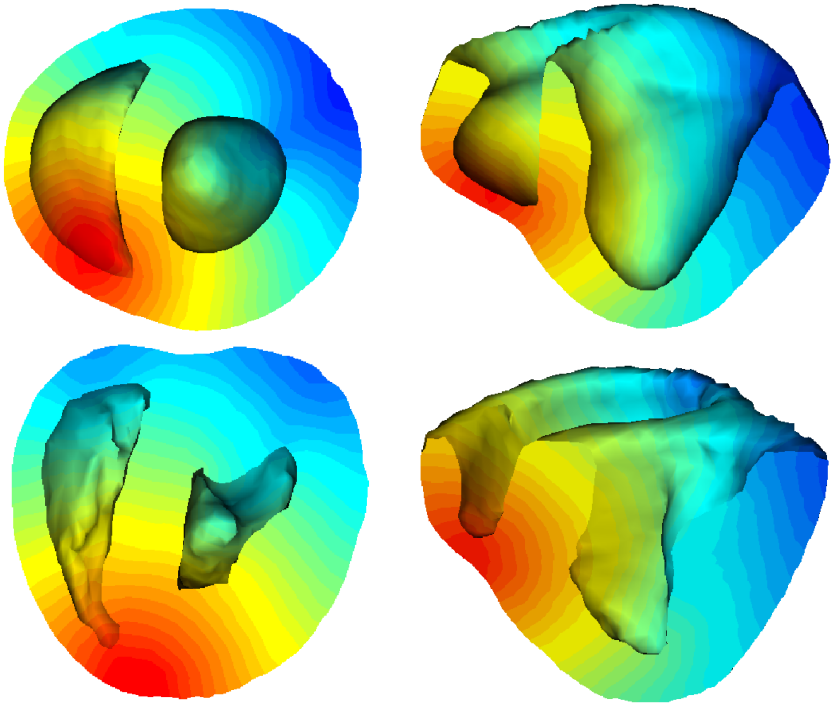

Fig. 11. Simulated Action Potential isochrones, visualized in the myocardium wall, for the UCSD model simulations (top row) and for the DTI model simulations (bottom row).